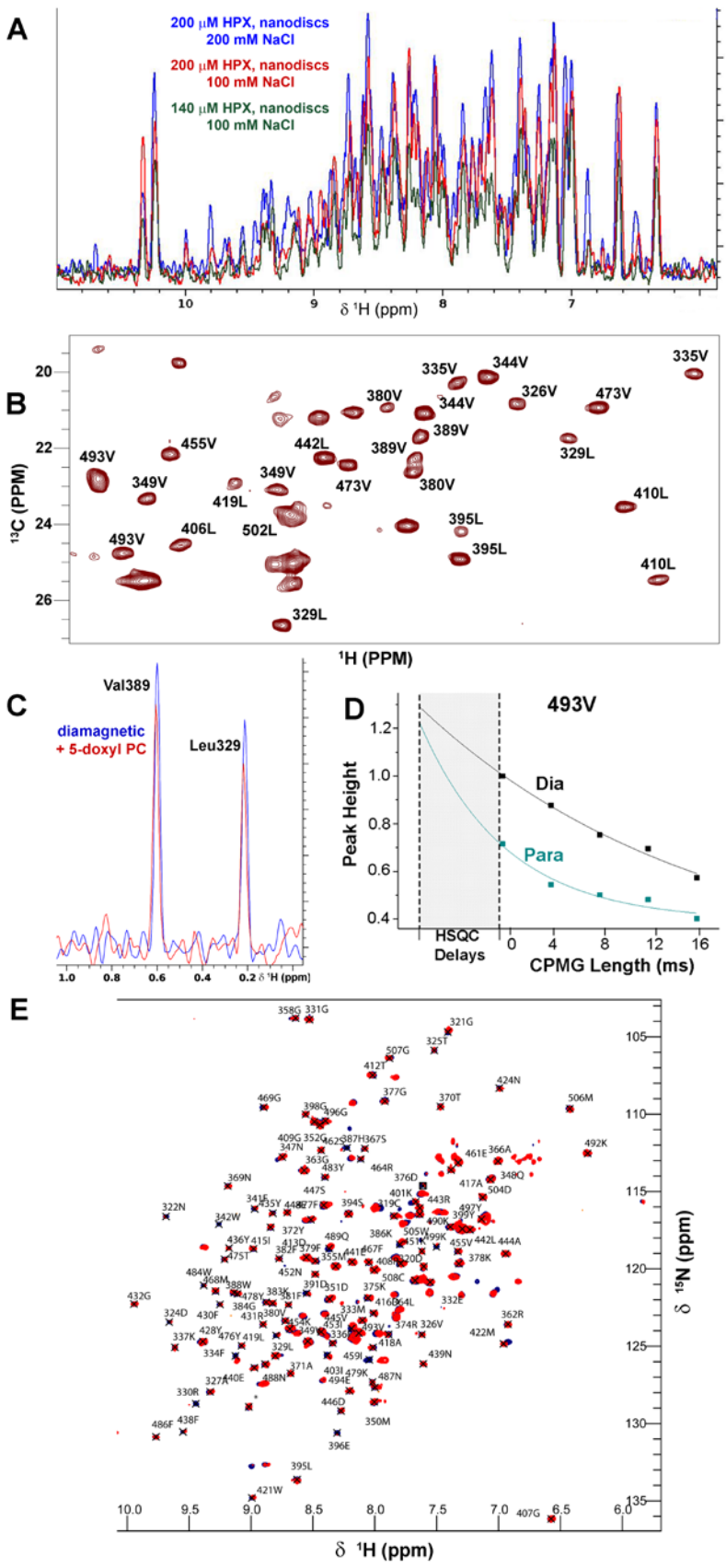
A
200 μM HPX, nanodiscs
200 mM NaCl
200 μM HPX, nanodiscs
100 mM NaCl
140 μM HPX, nanodiscs
100 mM NaCl
δ ¹H (ppm)
B
¹³C (PPM)
¹H (PPM)
C
Val389
diamagnetic
+ 5-doxyl PC
Leu329
δ ¹H (ppm)
D
493V
Peak Height
Dia
Para
HSQC
Delays
CPMG Length (ms)
E
δ ¹⁵N (ppm)
δ ¹H (ppm)

Figure S1. Related to Figure 1. Dependence of the NMR Spectra of the HPX Domain of MT1-MMP Mixed with Nanodiscs on Conditions and PREs.

(A) Increasing the concentrations of salt and binding partners improve the NMR spectra. ^{15}N-labeled HPX domain of MT1-MMP was mixed 1:1 with nanodiscs. 2D BEST-TROSY spectra (Lescop et al., 2010) were acquired in 34 min. at 800 MHz, 30°C in 20 mM Tris (pH 7.4) in a 3 mm tube. Skyline projections of them are plotted. Peak heights at 300 mM NaCl were similar to those at 200 mM NaCl (spectrum not shown).

(B) The Leu/Val methyl region of the ^{13}C HMQC spectrum of the HPX domain mixed 1:1 with nanodiscs (80 μM each) in 300 mM NaCl, pH 7.2.

(C) A 1D slice through the ^{13}C HMQC spectra without (blue) and with the 5-doxyl PC (red) added to the nanodiscs shows the weakening of two methyl peaks that experience paramagnetic relaxation by the probe.

(D) The NMR relaxation decays defining Γ_2 (the PRE) at Val493 are shown in the presence of paramagnetic and diamagnetic nanodiscs. The peak heights are measured as a function of the length of the CPMG portion of the NMR pulse sequence.

(E) ^{15}N TROSY spectra of the HPX domain before (red) and after addition of nanodiscs (blue). The NMR peak assignments are available at the BioMagResBank under accession code 25048.

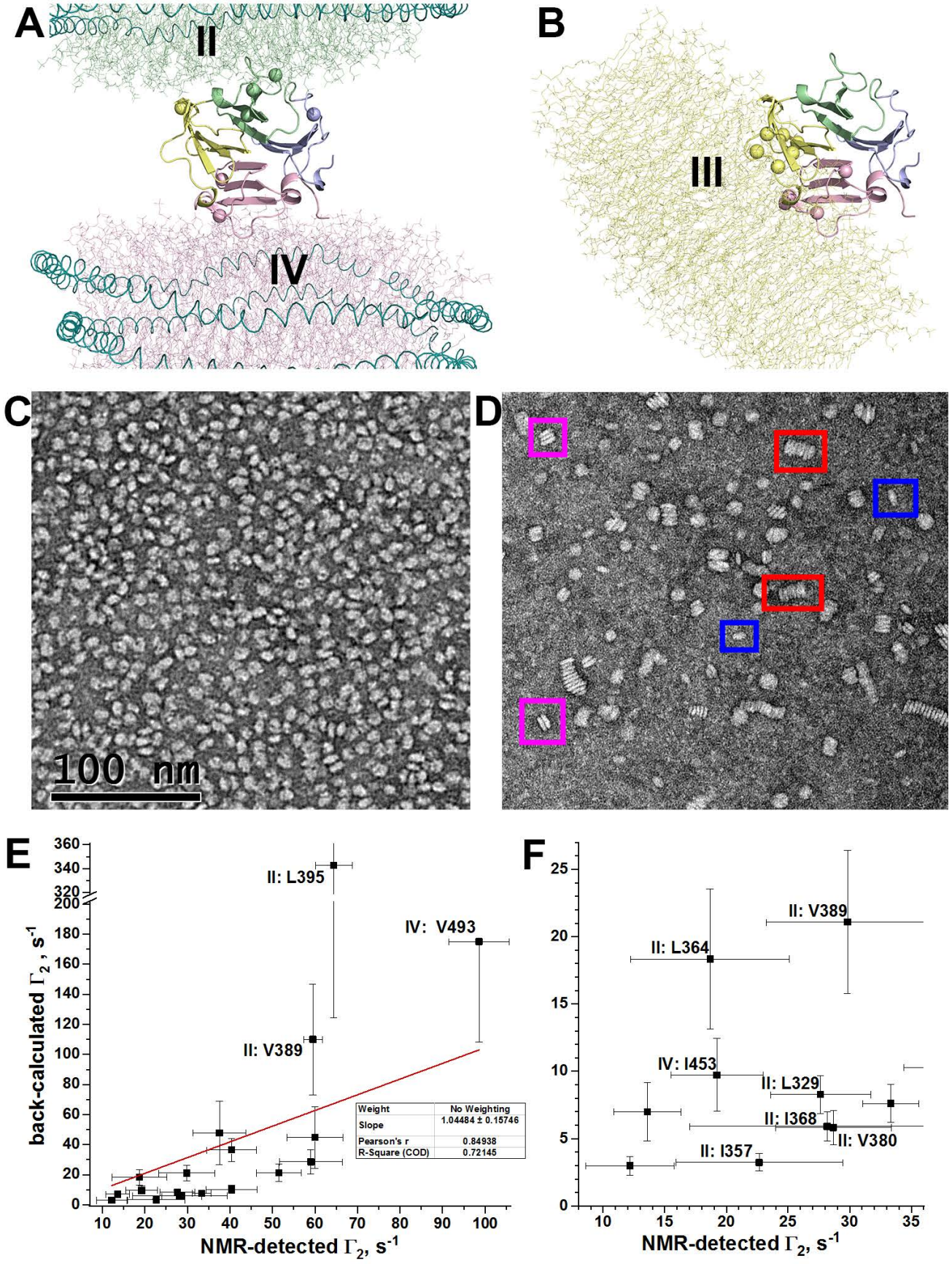
A
II
IV
B
III
C
100 nm
D
E
back-calculated Γ2, s-1
NMR-detected Γ2, s-1
II: L395
IV: V493
II: V389
Weight
No Weighting
Slope
1.04484 ± 0.15746
Pearson's r
0.84938
R-Square (COD)
0.72145
F
NMR-detected Γ2, s-1
II: V389
II: L364
IV: I453
II: L329
II: I368
II: V380
II: I357

Figure S2. Related to Figure 2. Spectroscopy and Negative Staining Electron Microscopy Imply Two Peripheral Membrane Binding Surfaces on Soluble MT1-MMP.

(A) Both modes of peripheral membrane binding by the HPX domain discovered by paramagnetic NMR and fluorescence proximity assays are superimposed. The blade II-proximal association colors lipids in green. The blade IV-proximal association colors lipids in pink.

(B) The recent proposal of binding instead at blade III (Cerofolini et al., 2016) is plotted with the HPX domain in the same orientation in order to illustrate the difference in orientation from the orientations suggested by the evidence herein. Blade III is colored yellow.

(C) An image from electron microscopy is shown of DMPC nanodiscs (0.7 μM at application) negatively stained with methylamine tungstate (Nano-W®).

(D) A Nano-W-stained image from electron microscopy is shown of mixtures of sMT1-MMP with nanodiscs, each around 1 μM when incubated with the grid (without NaCl). Single nanodiscs are outlined in blue, stacked nanodiscs in pink, and higher order stacking in red.

(E) PREs back-calculated from the coordinates of the HPX-nanodisc complexes are plotted vs. Γ_2 relaxation rate constants measured by NMR. Measured Γ_2 values that are at least 2-fold greater than fitting uncertainties are plotted. The uncertainties in the back-calculated Γ_2 values result from variation the distance from bilayer to methyl groups among the 15 members of each structural ensemble, with SD of 0.9 Å on average. Methyl groups in the coordinates that are slightly closer to the nanodiscs than suggested by measured Γ_2 are labeled by residue. The II: prefix to residue labels refers to that residue in the ensemble with blade II inserting into the nanodisc. The IV: prefix likewise refers to the ensemble with blade IV inserted. The deviating L395 point was omitted from the linear fit plotted.

(F) The region of small PREs from the plot of (E) is expanded here. Methyl groups with Γ_2 values not used as distance restraints because they are < 30 s^{-1}, but which are experimentally significant nonetheless, are labeled by residue.

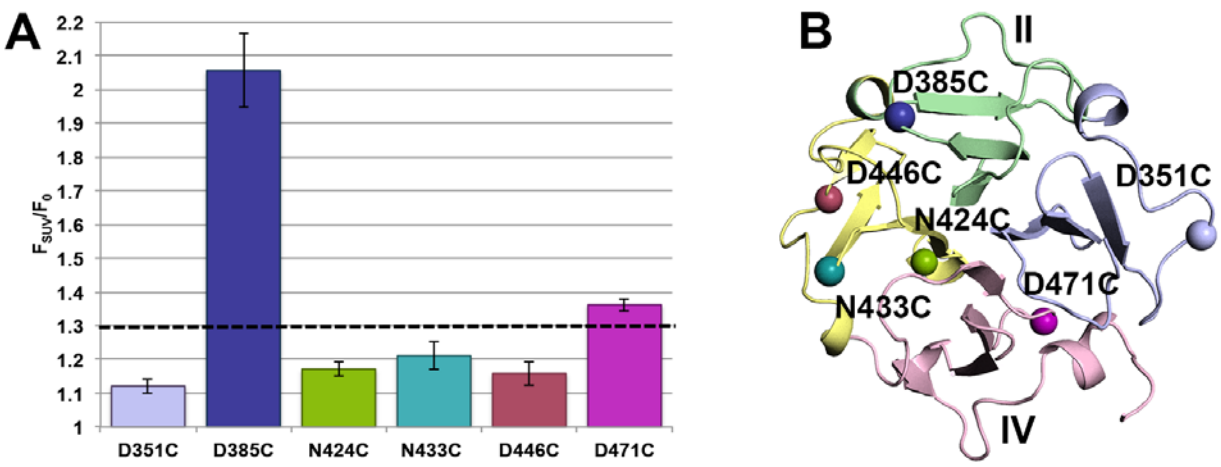

Figure S3. Related to Figure 3. Site-Directed Fluor Labeling Confirms the Proximity to DMPC Vesicles of Blades II and IV and Disputes the Proximity of Blades I and III

The polarity-sensitive fluorophore IANBD was conjugated to a single cysteine substitution at each of six sites on the HPX domain of MT1-MMP.

(A) The fluorescence emission of IANBD in the presence of SUVs is normalized by that in the absence. Increases of fluorescence emission of 1.3-fold or greater are considered evidence of the exposed NBD groups dipping into a hydrophobic phase such as the acyl chains of a lipid bilayer. The uncertainties plotted are the SD of triplicate measurements.

(B) The sites of single cysteine substitutions are marked by spheres on the crystal structure (PDB: 3C7X).

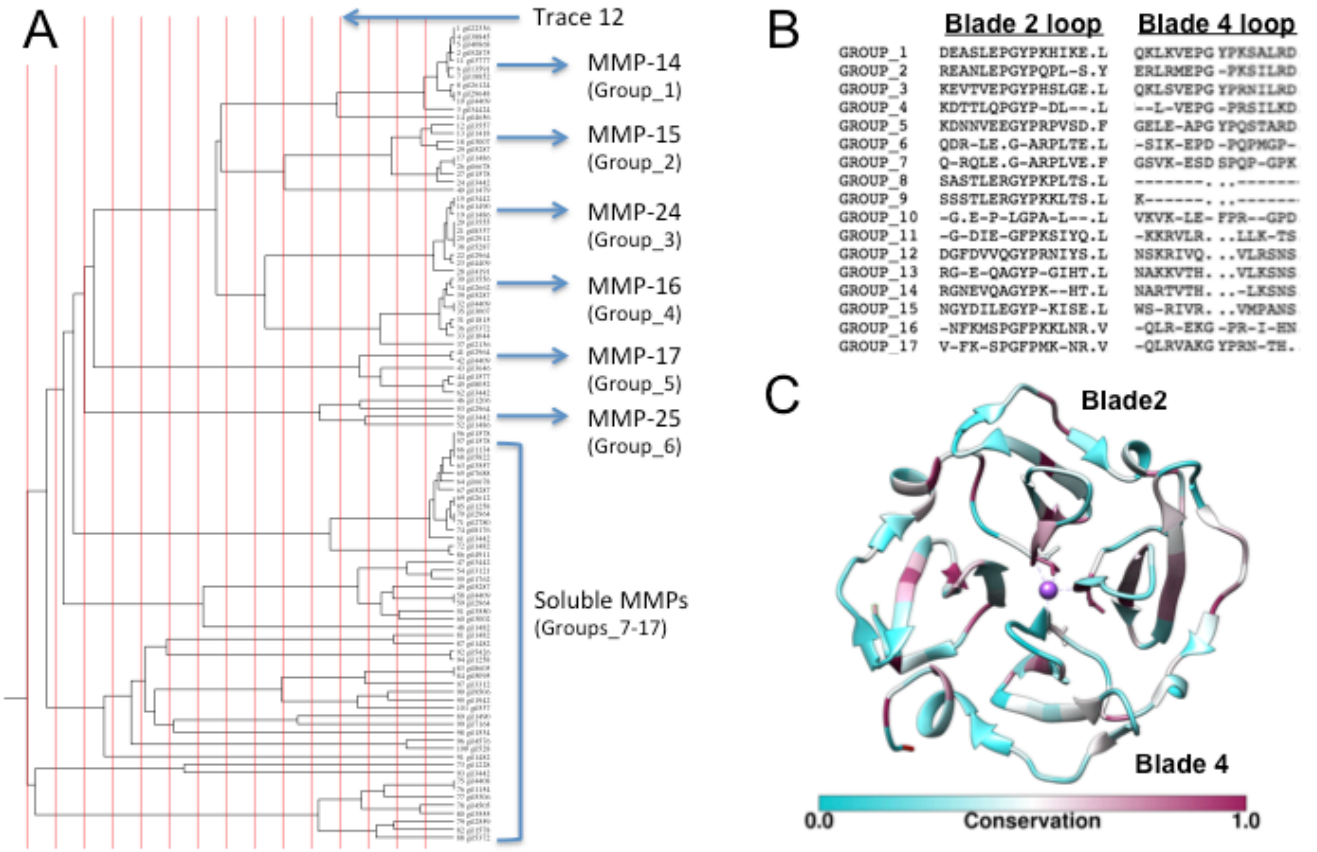

Figure S4. Related to Figure 3. Evolutionary Trace Analysis of MMP HPX Domains Reveals that MT MMPs with Transmembrane Helices Conserve the PGYP Sequence Motif in Blades II and IV.

This includes the EPGYPK loops of MT1-MMP that insert into nanodisc bilayers.

(A) The phylogenetic tree of aligned sequences from MMPs spanning 10 species of vertebrates.

(B) “Consensus sequences” conserved within subfamilies of MMPs are listed. The sequences are divided into subfamilies at the sequence identity cutoff named Trace level 12 which is pointed out by the arrow in panel A to the 12th vertical line from the left.

(C) Coloration of the conservation on the HPX structure from MT1-MMP indicates the second proline in the EPGY**P**K loop of blade II (pink) to be conserved over almost all MMPs.

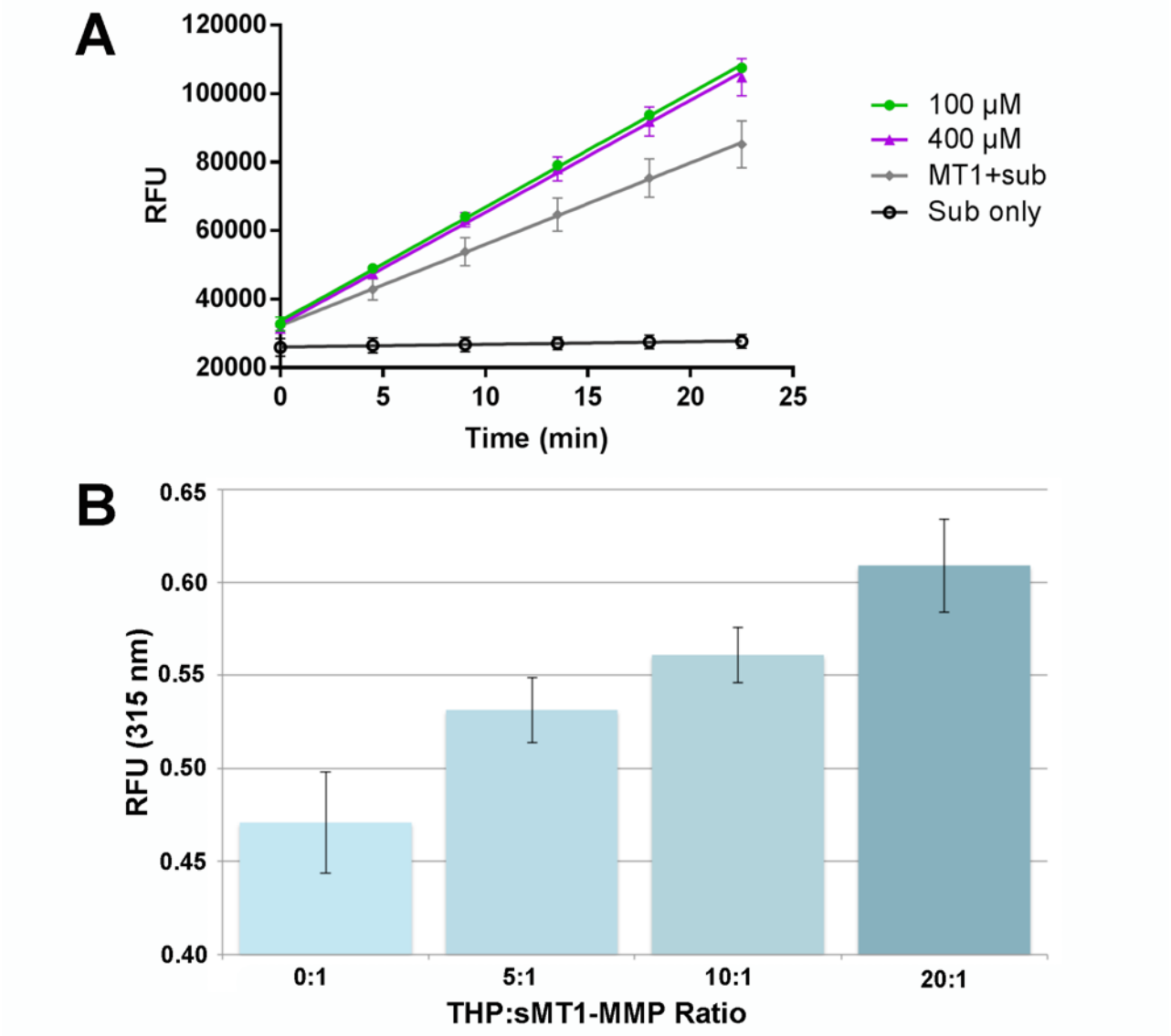

Figure S5. Related to Figure 4. Interplay between Vesicle and Collagen Triple-Helical Peptide Interactions with sMT1-MMP

(A) Additions of SUVs enhance hydrolysis of the fTHP-9 substrate. The amount of DMPC monomers present is given in the legend.

(B) Excess THP competes with SUVs for binding sMT1-MMP. Trp fluorescence emission is plotted on the ordinate and all measurements are normalized to free sMT1-MMP emission. The mole ratio of triple-helical peptide, α1(I)772–786 THP, to sMT1-MMP is indicated. Higher emission at 315 nm indicates less proximity to the pyrene quencher placed in the SUVs. The SUVs present throughout were composed of DMPC monomers at 250 µM with the addition of Pyrene-PE at 5 µM to quench the Trp fluorescence emission. The uncertainties plotted are the SD of triplicate measurements.

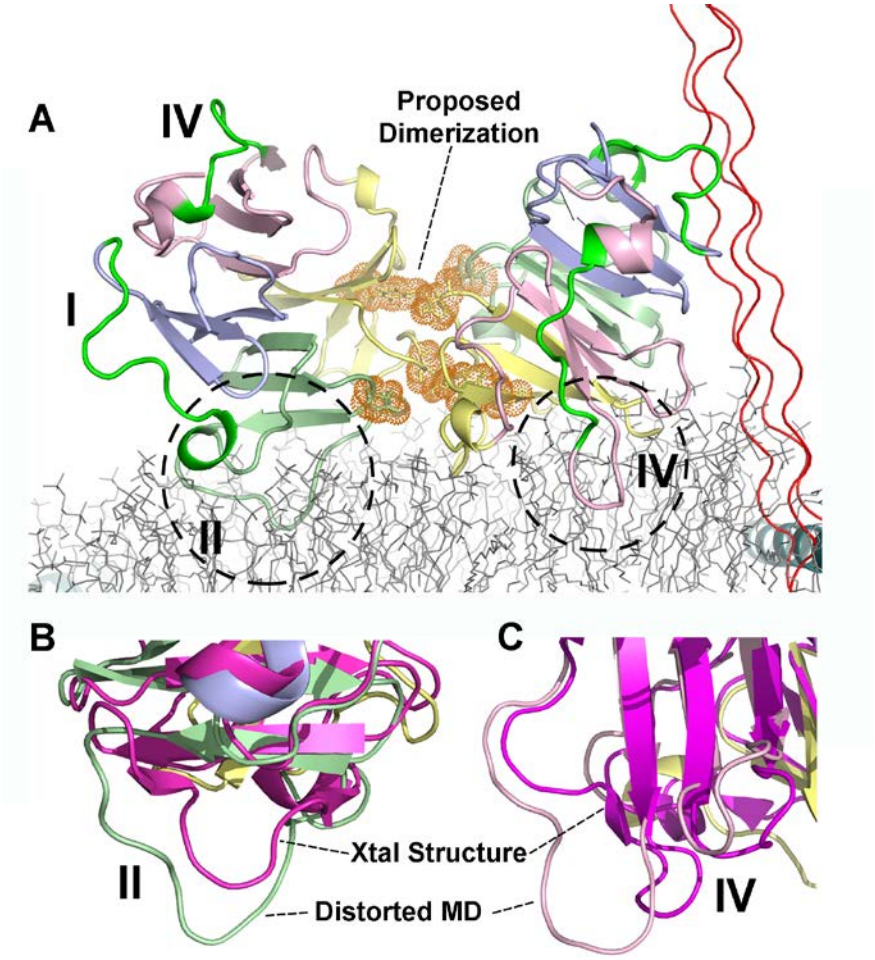

Figure S6. Related to Figure 5. Restrained MD Attempts to Satisfy the PRE-Based Distance Restraints of Nanodiscs to Both Blades II and IV of the Symmetric (V-shaped) Dimer Distort Both EPGYPK Membrane-Binding Loops.

(A) The lowest energy structure after 3 ns of minimization and equilibration with the PRE NMR-based distance restraints is plotted. Residues mutated in one study (Tochowicz et al., 2011) are highlighted with orange dots. Epitopes targeted by peptide inhibitors in another study are colored bright green (Zarrabi et al., 2011). The path of collagen triple-helix binding to the HPX domain alone (Zhao et al., 2015) is indicated by the triple-helix plotted with red ribbon.

(B) The distortion of blade II by the restrained MD is shown by the overlay of the structural model from (A; blade II in light green) with the crystallographic starting coordinates (PDB: 3C7X) in magenta.

(C) The distortion of blade IV is shown by the overlay of the outcome of the same restrained MD simulation (blade IV in light pink) with the crystal structure (magenta).

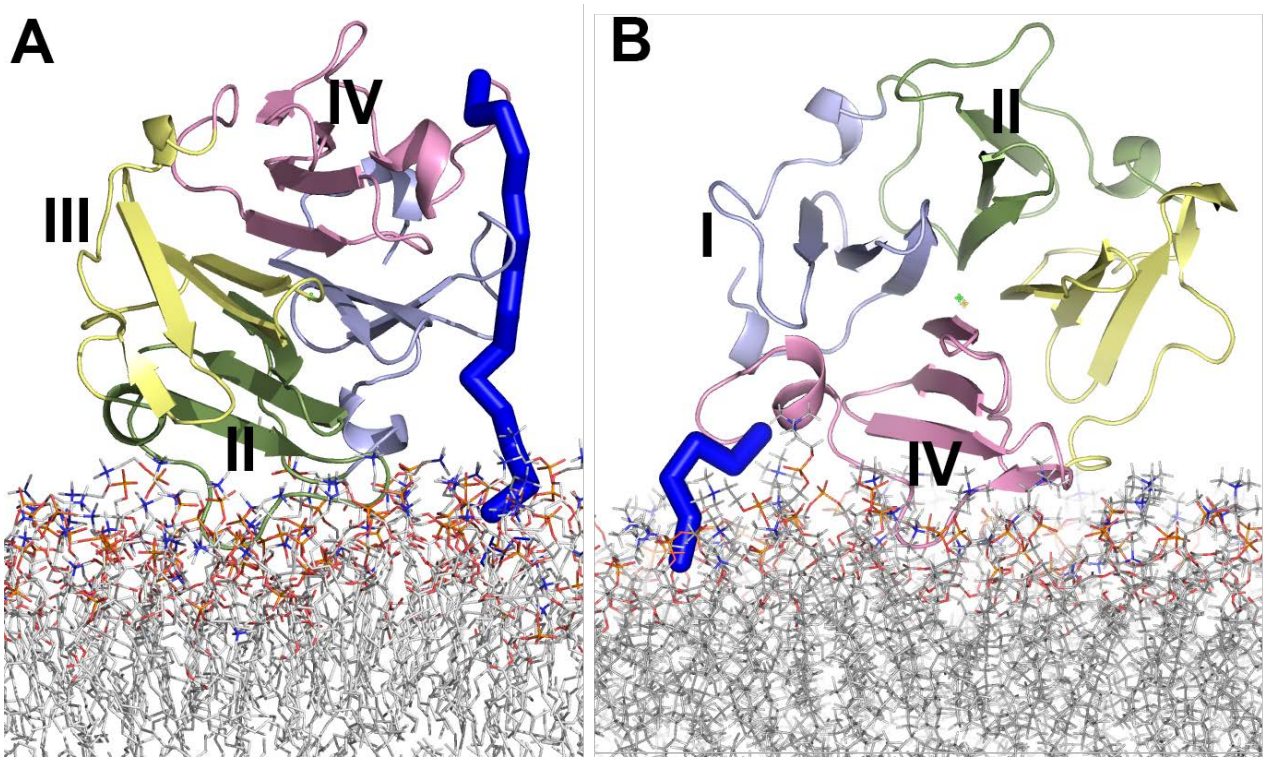

Figure S7. Related to Figure 5. Linker Segments Are Long Enough to Span from the HPX Domain to Bilayers, and Quite Possibly to the Transmembrane Helix as well.

(A) The coordinates with blade II bound to the nanodisc are plotted with 14 residues from a model of the linker-2 sequence of MT1-MMP built in extended conformation, minimized, and subjected to 1.5 ps of dynamics using Sybyl X 2.1.1 (Tripos). Manual docking (using Pymol) suggests 14 residues are capable of spanning the distance to the nanodisc surface.

(B) The coordinates with blade IV bound to the nanodisc are plotted with a 6 residue portion of the linker-2 sequence, easily reaching the surface of the model of the nanodisc.